Polyhedron 34 (2012) 181–187

Contents lists available at SciVerse ScienceDirect

Polyhedron

journal homepage: www.elsevier.com/locate/poly

Transition metal complexes of new glyoxylato-aroylhydrazones and their role in L-ascorbic acid oxidation inhibition

Róbert Csonka [a], Carolina Villalonga-Barber [a], Vassilis Psycharis [b], Catherine P. Raptopoulou [b], Barry R. Steele [a,*]

[a] Institute of Organic and Pharmaceutical Chemistry, National Hellenic Research Foundation, 48. Vas. Constantinou Ave., 11635 Athens, Greece
[b] Institute of Materials Science, NCSR Democritos, 15310 Aghia Paraskevi Attikis, Greece

ARTICLE INFO

Article history:
Received 18 November 2011
Accepted 24 December 2011
Available online 10 January 2012

Keywords:
Hydrazone complex
Glyoxylato-aroylhydrazone
Ascorbate oxidase
Ascorbate peroxidase
X-ray crystal structure
Iron
Copper
Zinc

ABSTRACT

We report here the synthesis of new ligands of the aroylhydrazone family. Glyoxylato-aroylhydrazones (gly-AH) with lipophilic character were designed for possible biological applications where metal chelation is desired. They were found to coordinate readily with a number of metals and the crystal structures of the copper and zinc complexes, $M(py)_2L$ (M = Cu, Zn); LH_2 (**L2**) = *N*′-(2-hydroxy-3-(pentan-3-yl)benzylidene)-2-mesityl-2-oxoacetohydrazide have been determined. The complexes both display a distorted trigonal bipyramidal coordination geometry around the metals. Ascorbate oxidase and ascorbate peroxidase mimicking reactions were carried out to determine the ability of the title ligands to inhibit metal-induced oxidation of L-ascorbic acid *via* complexes generated *in situ*.

1. Introduction

Many metals play an important biological role but, in some cases, their overexpression or accumulation can cause problems. Iron and copper, for example, are directly implicated in mechanisms leading to oxidative stress which, in turn, is a key factor involved in the development of age-related disorders such as Alzheimer's disease, Huntington's disease, Parkinson's disease and Friedreich's ataxia. Zinc is another important trace metal. It is a co-factor or catalytic factor of numerous enzymes. In the brain, during normal neuronal activity, zinc is released into the synaptic cleft and keeping its balance is necessary to avoid toxic effects or even death [1,2].

One way to combat the effects of excess accumulation of metals is by their complexation and removal from the system. Much attention has been directed to the use of chelation therapy to control iron overload which can have a variety of causes such as an increase in iron absorption from the diet, hereditary haemochromatosis, administration of iron in transfusion-dependent anaemias or certain pathological conditions. Iron-chelation therapy originated with the application of desferrioxamine (DFO) which is still widely used [1]. However, the poor membrane permeability of the hydrophilic DFO severely limits its ability to access intracellular iron or to cross the blood brain barrier. If a drug cannot cross the cell membranes, this implies a short excretion time and a shorter time for it to act [3]. Frequent drug administration can also be rather inconvenient for patients suffering from iron overdose diseases and these disadvantages have led to research into new potential iron-chelating ligands.

In the case of the above-mentioned diseases, the metal level in the brain is highly elevated. This state creates good conditions for Haber–Weiss type reactions (superoxide-driven Fenton chemistry [4]) that result in the production of reactive oxygen species (ROS). These radicals or radical anions are very powerful cell damaging factors that target lipids, proteins and DNA [5]. Under normal circumstances, excess levels of ROS can be dealt with by the living organism's own defense system which involves enzymes such as ascorbate peroxidase (APX) and ascorbate oxidase (AO). These catalyse the destruction of reactive oxygen species using smaller organic substrates such as L-ascorbic acid. The reaction mechanism of APX occurs *via* an electron transfer pathway where radicals are formed [6]. The presence of the semidehydroascorbate radical was observed during the AO process as well [7,8]. When metal concentrations are excessive, however, the normal defense mechanism is not sufficient and the study of potential metal chelators which can pass the blood brain barrier and irreversibly bind the metal is therefore of great interest. The aim of this study was the synthesis

* Corresponding author.
E-mail address: bsteele@eie.gr (B.R. Steele).

0277-5387/$ - see front matter © 2012 Elsevier Ltd. All rights reserved.
doi:10.1016/j.poly.2011.12.036

of a new lipophilic ligand type, which we term glyoxylato-aroylhydrazones (gly-AH), the structural description of new gly-AH complexes and the testing of the activity of these ligands in APX and AO mimicking reactions.

2. Materials and methods

2.1. Materials

The solvents and chemicals used for synthesis were purchased from Sigma–Aldrich and Alpha Aesar. DFO (desferrioxamine) was purchased from Novartis Pharma AG, Basel, Switzerland. They were used without further purification. Spectrograde solvents were used for the recording of UV–Vis spectra.

2.2. Analytical measurements

Infrared spectra were recorded on a Bruker Tensor 27 spectrophotometer using an ATR (attenuated total reflectance) assembly. UV–Vis spectra were recorded on a Cary 100 Conc spectrophotometer using quartz cells. ESI-MS spectra were recorded by a Thermo LCQ Fleet instrument. NMR spectra were recorded using Varian 300 and 600 MHz instruments.

2.3. Synthesis of glyoxylato-aroylhydrazones

2.3.1. Two procedures were used for the preparation of hydrazides

Method A (via acid chloride): Substituted arylglyoxylic acid (5 mmol) was dissolved in 10 ml $SOCl_2$ and the solution was heated at reflux temperature overnight. Excess $SOCl_2$ was removed by rotary evaporation and the crude product was dried under vacuum to yield substituted arylglyoxylic acid chlorides (95–98% light yellow oils) without further purification. A solution of the acid chloride (5 mmol) in CH_2Cl_2 (15 ml) was added dropwise over 40 min to a solution of hydrazine-hydrate (3 ml, 30 w/v% hydrazine-hydrate in 15 ml EtOH) cooled in an ice bath. Upon addition, the mixture was stirred at room temperature for 1 h. The crude precipitate was filtered and washed with saturated $NaHCO_3$, hexane and then finally dried under vacuum. Yield: 60–70% white powder.

Method B (via ester): The methyl ester of the corresponding arylglyoxylic acid can be prepared very rapidly using diazomethane [9]. The ester (0.4 g (approx. 2 mmol)) is converted to the hydrazide using an excess of 30 w/v% hydrazine-hydrate (1 ml dissolved in 15 ml EtOH or MeOH) with sonication for 20 min at 40 kHz in an ultrasonic bath. The precipitate formed was filtered, washed with EtOH and dried under vacuum. Yield: 75–95% white powder.

2.3.2. The preparation of glyoxylato-aroylhydrazones (*L1*–*L3*)

A solution of the corresponding hydrazide (1 mmol) and 3-(1-ethylpropyl)-2-hydroxybenzenecarbaldehyde (1.05 mmol) [10] in methanol was heated at reflux temperature overnight. The solvent was then removed by rotary evaporation and the remaining powder was washed with hexane, filtered and dried under vacuum to yield the corresponding glyoxylato-aroylhydrazones as light yellow powders (45–87%).

*2.3.2.1. (**L1**) (E)-N′-(2-hydroxy-3-(pentan-3-yl)benzylidene)-2-oxo-2-(2,4,6-triisopropylphenyl)-acetohydrazide.* Mp.: 171 °C. ^{1}H NMR (300 MHz, DMSO) δ (ppm): 12.81 (s, 1 H), 11.63 (s, 1 H), 8.73 (s, 1 H), 7.25 (m, 2 H), 7.12 (s, 2 H), 6.94 (t, *J* 7.0, 1 H), 3.00–2.85 (m, 2 H), 2.66–2.55 (m, 2 H), 1.71–1.49 (m, 4 H), 1.23 (d, *J* 7.0, 6 H), 1.16 (d, *J* 7.0, 12 H), 0.72 (t, *J* 7.0, 6 H); ^{13}C NMR (75 MHz, DMSO) δ (ppm): 12.4, 24.2, 24.2, 27.7, 31.4, 34.2, 40.7, 117.4, 119.8, 121.2, 129.7, 130.7, 132.8, 145.8, 151.0, 154.7, 156.7, 158.0, 198.2. IR (ATR) (cm^{-1}): 3166, 3031, 2963, 2927, 2872, 1685, 1665, 1605, 1534, 1459, 1439, 1364, 1273, 1225, 1099, 1012, 972, 857, 825, 750. ESI-MS (DCM/MeOH): *m/z* (%) = 487.20 [M+Na$^+$]. Molecular formula: $C_{29}H_{40}N_2O_3$. Molecular weight: 464.64 g/mol.

*2.3.2.2. (**L2**) (E)-N′-(2-hydroxy-3-(pentan-3-yl)benzylidene)-2-mesityl-2-oxoacetohydrazide.* Mp.: 149–151 °C. ^{1}H NMR (300 MHz, DMSO) δ (ppm): 12.78 (s, 1 H), 11.64 (s, 1 H), 8.69 (s, 1 H), 7.27 (d, *J* 8.0, 1 H), 7.23 (d, *J* 8.0, 1 H), 6.96 (m, 3 H), 3.00–2.86 (m, 1 H), 2.83 (s, 3 H), 2.17 (s, 6 H), 1.74–1.43 (m, 4 H), 0.72 (t, *J* 7.0, 6 H); ^{13}C NMR (150 MHz, DMSO) δ (ppm): 12.4, 19.6, 21.2, 27.7, 40.7, 117.4, 119.7, 129.0, 129.6, 130.7, 132.8, 135.8, 140.5, 154.5, 156.7, 158.7, 196.3. IR (ATR) (cm^{-1}): 3186, 3051, 2964, 2933, 2873, 1695, 1675, 1604, 1549, 1453, 1379, 1268, 1232, 1209, 1157, 1091, 975, 833, 754, 702. ESI-MS (DCM/MeOH): *m/z* (%) = 403.10 [M+Na$^+$]. Molecular formula: $C_{23}H_{28}N_2O_3$. Molecular weight: 380.48 g/mol.

*2.3.2.3. (**L3**) (E)-2-(4-(dimethylamino)phenyl)-N′-(2-hydroxy-3-(pentan-3-yl)benzylidene)-2-oxoacetohydrazide.* Mp.: 231–232 °C. ^{1}H NMR (600 MHz, DMSO) δ (ppm): 12.54 (s, 1 H), 11.78 (s, 1 H), 8.53 (s, 1 H), 7.96 (d, *J* 9.0, 2 H), 7.25 (d, *J* 7.0, 1 H), 7.22 (d, *J* 7.0, 1 H), 6.93 (t, *J* 7.0, 1 H), 6.80 (d, *J* 9.0, 2 H), 3.10 (s, 6 H), 3.00–2.92 (m, 1 H), 1.74–1.51 (m, 4 H), 0.75 (t, *J* 7.0, 6 H); ^{13}C NMR (75 MHz, DMSO) δ (ppm): 12.4, 27.8, 40.1, 111.4, 117.5, 119.6, 120.2, 129.5, 130.5, 132.7, 152.8, 154.8, 156.7, 161.7, 185.9. IR (ATR) (cm^{-1}): 3277, 3240, 2962, 2931, 2870, 1693, 1664, 1574, 1505, 1440, 1382, 1305, 1167, 947, 836, 751, 621. ESI-MS (MeOH): *m/z* (%) = 404.10 [M+Na$^+$]. Molecular formula: $C_{22}H_{27}N_3O_3$. Molecular weight: 381.47 g/mol.

2.4. Synthesis of transition metal complexes of glyoxylato-aroylhydrazones

$Cu(OAc)_2{\cdot}2H_2O$ or $Zn(OAc)_2{\cdot}2H_2O$ (2 mmol) was added to a solution of gly-AH ligands (2 mmol) in a methanol–pyridine (1:1) mixture (5 ml). After stirring for 5 min the solution was then left

Table 1
Summary of the crystallographic data and structure parameters for **C1** and **C2**.

Compound	**C1**	**C2**
Chemical formula	$C_{33}H_{36}CuN_4O_3$	$C_{33}H_{36}N_4O_3Zn$
Formula weight	600.20	602.03
Crystal system	triclinic	triclinic
Space group	$P\bar{1}$	$P\bar{1}$
Unit cell dimensions		
a (Å)	8.5089(1)	8.3443(1)
b (Å)	14.1869(2)	14.1889(2)
c (Å)	14.4149(3)	14.3665(3)
α (°)	110.281(1)	108.935(1)
β (°)	102.053(1)	100.465 (1)
γ (°)	104.001(1)	104.421(1)
Volume (Å^3)	1499.60(4)	1492.89(4)
Z	2	2
Calculated density (g cm^{-1})	1.329	1.339
Temperature (K)	183(2)	160(2)
Absorption coefficient (mm^{-1})	1.342	1.458
F (000)	630	632
Observed reflections	4548	4465
Goodness-of-fit (GOF) on F^2	1.028	1.050
Final *R* indices [$I > 2(I)$][a]	R_1 = 0.0471, wR_2 = 0.1253	R_1 = 0.0312, wR_2 = 0.0805

[a] $w = 1/[\sigma^2(F_0^2) + (\alpha P)^2 + bP]$ and $P = ((\max F_0^2, 0) + 2F_c^2)/3$.$R_1 = \sum(|F_0| - |F_c|)/\sum(|F_0|)$ and $wR_2 = \{\sum[w(F_0^2 - F_c^2)^2]/\sum[w(F_0^2)^2]\}^{1/2}$.

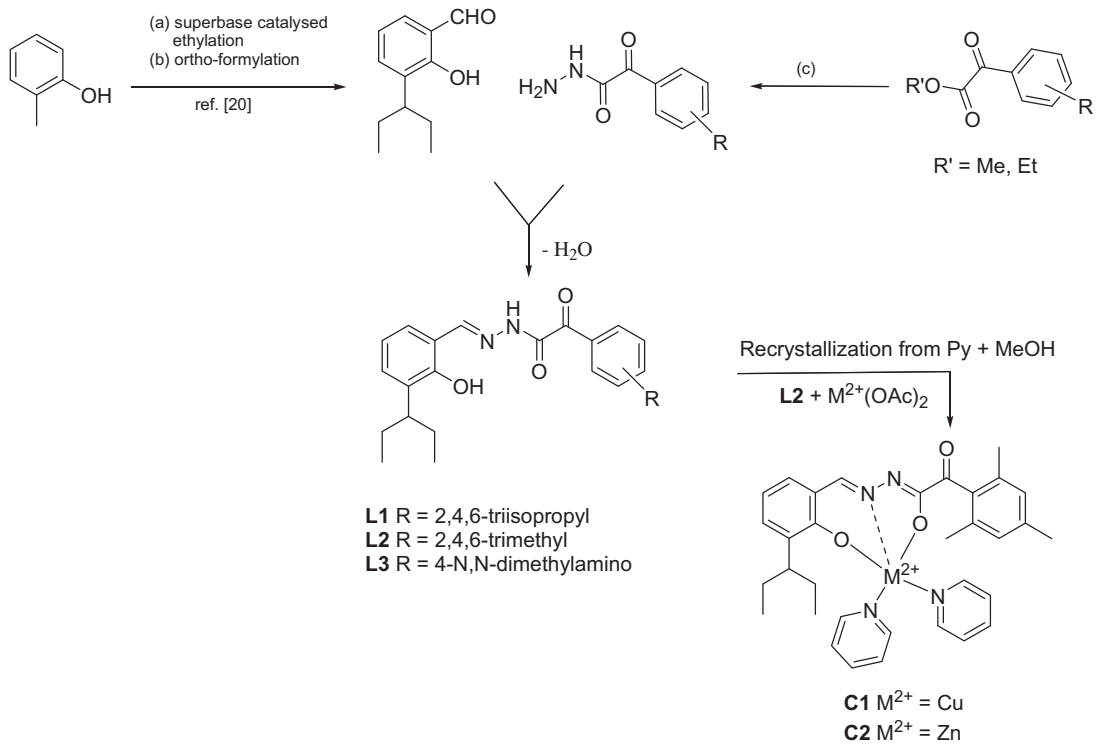

Scheme 1. Scheme of the synthesis of gly-AHs and their complexes. *Conditions:* (a) *n*BuLi, $LiK(OCH_2CH_2NMe_2)_2$, $Mg(OCH_2CH_2OEt)_2$, C_2H_4, 10 atm, 80 °C; (b) $(CH_2O)_n$, $MgCl_2$, NEt_3; (c) $NH_2NH_2{\cdot}xH_2O$, EtOH, 20 min sonication in ultrasonic bath.

Table 2
Analytical and physical data for the ligands and their metal(II) complexes.

Lig. and Comp.	Formula	Color	mp (°C)	UV log ε	ESI-MS *m/z* (%)
L1	$C_{29}H_{40}N_2O_3$	Light yellow	171	ε_{307} = 3.48 ε_{220} = 3.62	487.20 [M+Na$^+$]
L2	$C_{23}H_{28}N_2O_3$	Light yellow	149–151	ε_{298} = 4.20 ε_{223} = 4.21	403.10 [M+Na$^+$]
L3	$C_{22}H_{27}N_3O_3$	Dark yellow	231–232	ε_{362} = 3.35 ε_{289} = 3.10	404.10 [M+Na$^+$]
C1	$C_{33}H_{36}CuN_4O_3$	Dark green	>250	ε_{421} = 3.33 ε_{297} = 3.40	601.01 [M+H$^+$]
C2	$C_{33}H_{36}N_4O_3Zn$	Orange	>250	ε_{422} = 4.04 ε_{323} = 3.92	603.07 [M+H$^+$]

Table 3
IR spectral (cm^{-1}) assignment for the ligands and their metal(II) complexes.

	ν(O–H)	*ν*(N–H)	*ν*(C–H)	*ν*(C=O)	*ν*(C=N)
L1	3166	3031	2963, 2927, 2872	1685, 1665	1534
L2	3186	3051	2964, 2933, 2873	1695, 1675	1549
L3	3240	3277	2962, 2931, 2870	1693, 1664	1574
C1	–	–	2962, 2927, 2871	1686	1538
C2	–	–	2963, 2931, 2871	1684	1538

to evaporate slowly over approximately one week. Green and orange crystals (**C1** and **C2** respectively) were obtained that were suitable for single crystal X-ray diffraction studies.

*2.4.1. (**C1**) Cu(**L2**)(Py)$_2$*

Mp.: >250 °C. IR (ATR) (cm^{-1}): 2962, 2927, 2871, 1686, 1606, 1539, 1447, 1423, 1372, 1336, 1205, 1157, 1069, 1038, 1010, 966, 871, 851, 747, 696, 624. ESI-MS (MeOH): *m/z* (%) = 601.01 [M+H$^+$]. Molecular formula: $C_{33}H_{36}CuN_4O_3$. Molecular weight: 600.21 g/mol.

*2.4.2. (**C2**) Zn(**L2**)(Py)$_2$*

Mp.: >250 °C. IR (ATR) (cm^{-1}): 2963, 2951, 2930, 2871, 1684, 1602, 1539, 1487, 1451, 1427, 1368, 1220, 1198, 1069, 1042, 1014, 974, 871, 751, 700, 632. ESI-MS (MeOH): *m/z* (%) = 603.07 [M+H$^+$]. Molecular formula: $C_{33}H_{36}N_4O_3Zn$. Molecular weight: 602.07 g/mol.

2.5. Description of the L-ascorbic acid oxidation inhibition reactions

For the investigation of the inhibition reactions low concentration (0.7–5 mM) stock solutions of the reagents were prepared. The different functional groups on the ligands (**L1–L3**) had no observable effect on the oxidation reactions so only **L2** was used for systematic studies. In a typical experiment, $FeCl_3$, $Cu(OAc)_2{\cdot}2H_2O$, or $Zn(OAc)_2{\cdot}2H_2O$ (5.57×10^{-8} mol), **L2** (or DFO or EDTA) (5.57×10^{-8} mol) and L-ascorbic acid (5.57×10^{-7} mol) (and

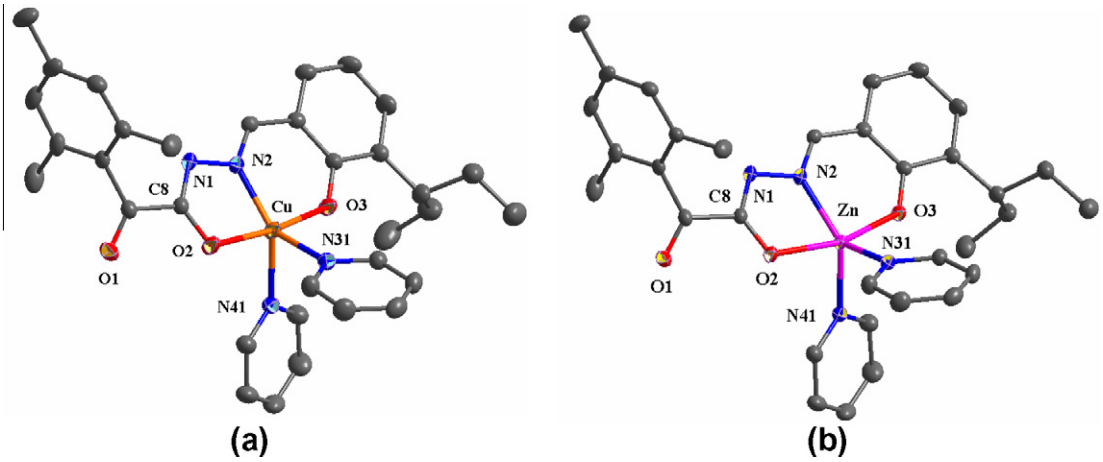

Fig. 1. Partially labeled plot of **C1** (a) and **C2** (b). Thermal ellipsoids are drawn at 30% probability level. Hydrogen atoms are omitted for clarity.

Table 4
Selected bond distances (Å) and angles (°) for **C1** and **C2**.

	Cu(**L2**)(Py)$_2$	Zn(**L2**)(Py)$_2$
M^{2+}–N(2)	1.932(2)	2.034(2)
M^{2+}–N(31)	2.190(2)	2.090(2)
M^{2+}–N(41)	2.123(2)	2.066(1)
M^{2+}–O(2)	1.974(2)	2.105(1)
M^{2+}–O(3)	1.914(2)	2.012(1)
N(2)–M^{2+}–N(31)	132.89(8)	131.51(6)
N(2)–M^{2+}–O(2)	80.78(8)	77.46(6)
N(2)–M^{2+}–O(3)	91.65(8)	87.75(6)
N(31)–M^{2+}–N(41)	87.87(7)	96.80(6)
O(2)–M^{2+}–O(3)	172.41(7)	165.21(5)
O(2)–M^{2+}–N(41)	92.18(8)	94.11(6)
O(3)–M^{2+}–N(41)	93.24(8)	95.73(6)
N(2)–M^{2+}–N(41)	138.64(8)	131.17(6)
O(3)–M^{2+}–N(31)	92.66(8)	94.99(6)
O(2)–M^{2+}–N(31)	92.84(8)	94.78(6)

equimolar H_2O_2 in case of $FeCl_3$) were taken from the stock solutions, mixed and diluted with methanol to 5 cm^3, in a volumetric flask. The oxidation reaction was followed by monitoring spectrophotometrically the decomposition of L-ascorbic acid (ε_{244} = 9539.95 M^{-1} cm^{-1} in methanol) at 244 nm as a function of time (λ_{max} of a typical band of L-ascorbic acid).

2.6. X-ray structure determination of Cu(*L2*)(Py)$_2$ (*C1*) and Zn(*L2*)(Py)$_2$ (*C2*)

Single crystals of **C1** and **C2** were obtained that were suitable for X-ray diffraction analysis. A crystal of **C1** (0.17 × 0.58 × 0.74 mm) and a crystal of **C2** (0.14 × 0.39 × 0.64 mm) were taken from the mother liquor and immediately cooled to −90 °C and −113 °C, respectively. Diffraction measurements were made on a Rigaku R-AXIS SPIDER Image Plate diffractometer using graphite monochromated Cu Kα radiation. Data collection (ω-scans) and processing (cell refinement, data reduction and Empirical absorption correction) were performed using the CrystalClear program package [11]. The structures were solved by direct methods using SHELXS-97 [12] and refined by full-matrix least-squares techniques on F^2 with SHELXL-97 [13]. Further experimental crystallographic details for **C1**: $2\theta_{max}$ = 130°; reflections collected/unique/used, 23 533/4826 [R_{int} = 0.0252]/4826; 375 parameters refined; $(\Delta/\sigma)_{max}$ = 0.001; $(\Delta\rho)_{max}/(\Delta\rho)_{min}$ = 0.928/−0.730 e/Å^3; R_1/wR_2 (for all data), 0.0487/0.1266. Further experimental crystallographic details for **C2**: $2\theta_{max}$ = 130°; reflections collected/unique/used, 23 393/4822 [R_{int} = 0.0269]/4822; 470 parameters refined; $(\Delta/\sigma)_{max}$ = 0.000; $(\Delta\rho)_{max}/(\Delta\rho)_{min}$ = 0.331/−0.300 e/Å^3; R_1/wR_2 (for all data), 0.0336/0.0815. Hydrogen atoms were introduced at calculated positions as riding on bonded atoms. All non-hydrogen atoms were refined anisotropically. Plots of all structures were drawn using the DIAMOND 3 program package [14] (Table 1).

3. Results and discussion

3.1. Ligand design

Aroylhydrazones (AH) are excellent multidentate ligands for transition metals. They have been shown to exhibit a range of biological activity such as DNA synthesis inhibition, or antiproliferative behavior [10,15,16]. Complex formation with different metals has also resulted in the discovery of compounds with interesting physical properties in the fields of nonlinear optics or magnetism [17–19]. Their properties can be tuned by modification of either the aldehyde or the carboxylic acid component and our aim was to increase lipophilicity using bulky aliphatic groups and to investigate the influence on the coordination sphere by the use of derivatives of arylglyoxylic acids instead of arenecarboxylic acids.

Scheme 1 shows synthetic routes leading to gly-AH type ligands and to their complexes. The superbase catalysed synthesis of sterically demanding aromatics has been described in earlier work of our group [20], while the subsequent steps were performed using standard procedures.

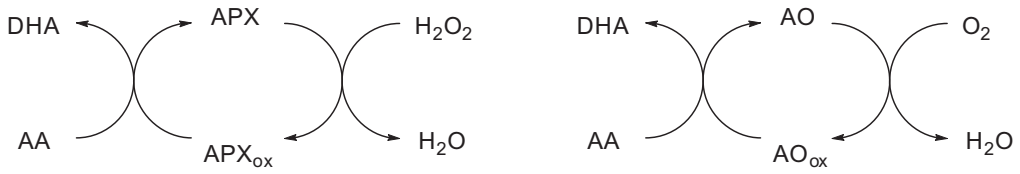

Fig. 2. The enzymatic cycle of APX and AO.

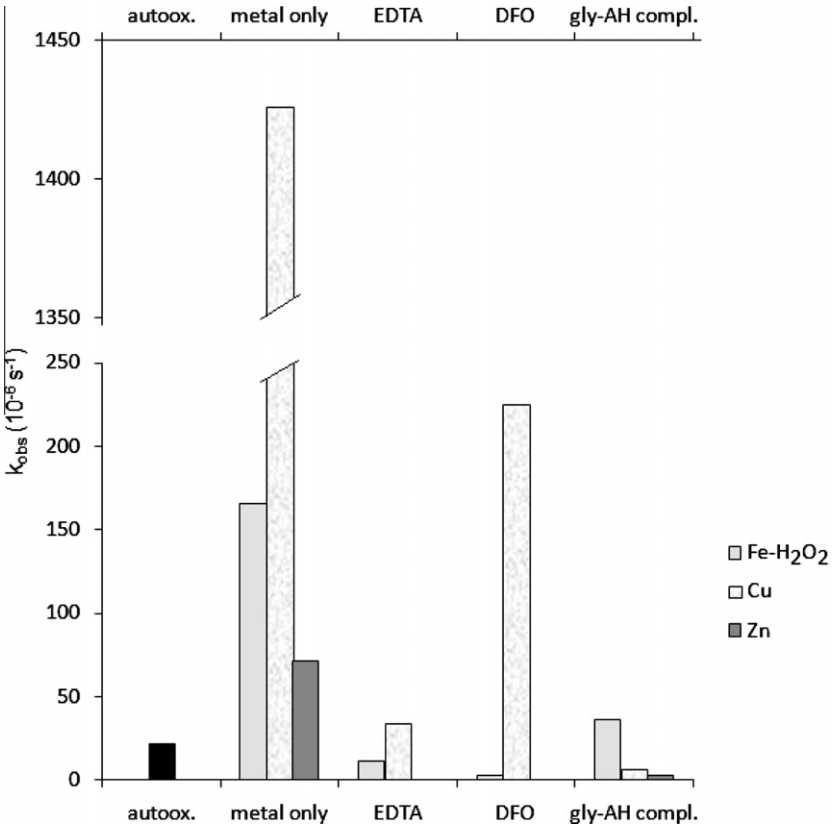

Fig. 3. The catalytic effect of metal salts and the inhibitory effect of **L2** complexes on AA oxidation. [Ascorbic acid]:[**L2**]:[$FeCl_3$, or $Cu(OAc)_2{\cdot}2H_2O$, or $Zn(OAc)_2{\cdot}2H_2O$] = 10:1:1 = 1.1×10^{-4} mol/dm^3:1.1×10^{-5} mol/dm^3:1.1×10^{-5} mol/dm^3; 25 °C, methanol.

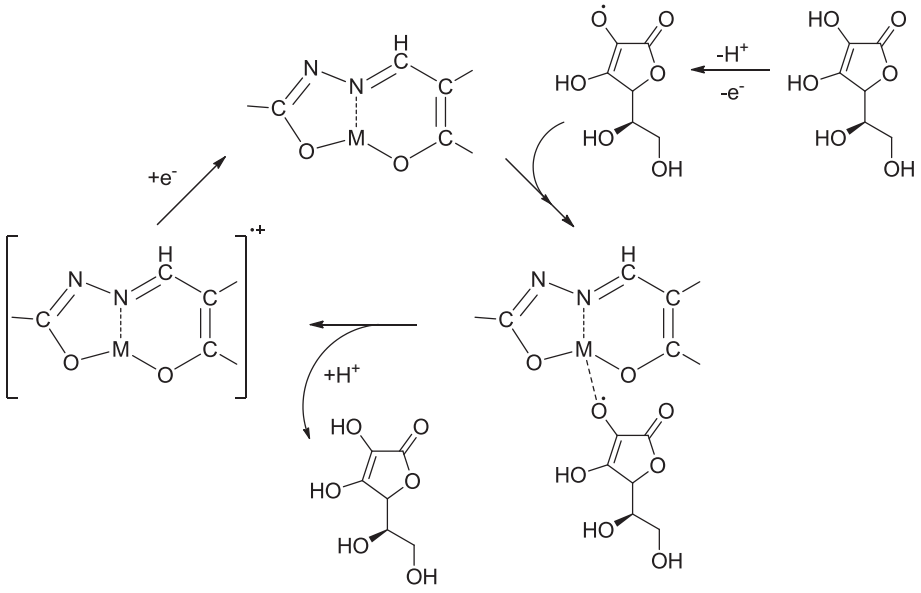

Scheme 2. The role of the tautomeric system of [M^{II}(gly-AH)](OAc) complexes in radical recombination.

3.2. Spectroscopic and single crystal X-ray structural characterization of ligand and complexes

3.2.1. UV–Vis and FT-IR

The gly-AH ligands show two strong absorption bands in the region of 250–400 nm in the electronic spectrum in methanol. This is the expected region for π–π^* and n–π^* transitions as found for other AH derivatives. For the complexes the absorption appears in the 350–450 nm region and can be assigned to ligand to metal charge-transfer transition (LMCT). Another CT band was also observed in the region 300–350 nm and can be attributed to O–metal(II) charge transfer as observed previously in other related zinc, cadmium and copper complexes [18,21] (Table 2).

The most characteristic vibration of gly-AH ligands in the infrared spectra is a strong double band between 1650 and 1700 cm^{-1} assigned to the ν(C=O) vibrations. Upon complex formation a

single peak is observed. Similarly to aroylhydrazones, the gly-AH compounds behave like tridentate ligands, therefore one free carbonyl vibration remains detectable. Another sign of complex formation is the disappearance of broad ν(OH) and ν(NH) peaks beyond 3000 cm^{-1}. There was no indication for coordinated water molecules in the structure. During chelate formation the ligand undergoes a keto-enol tautomerism and a remarkably strong peak appears around 1540 cm^{-1} due to ν(N=C–C=N) [22] (Table 3).

3.2.2. X-ray structures

Although there was ample evidence for complex formation by the simple addition of the ligands to solutions of the metal salts, crystals suitable for structure determination by X-ray diffraction could not be obtained. However using pyridine as a co-ligand it was possible to prepare suitable crystals of the complexes **C1** and **C2**. Partially labeled plots of the molecular structures of **C1** and **C2** are given in Fig. 1.

Both compounds are isomorphous, thus the coordination spheres around the metals are similar. They both show a distorted coordination geometry around the metal ion which is intermediate between square pyramidal and trigonal bipyramidal as evidenced by the value of the trigonality index $\tau = 0.56$ ($\tau = 0$ for ideal sq and $\tau = 1$ for ideal tbp) [23]. Other aroylhydrazone complexes that have been reported usually display distorted octahedral and square planar, [21,24,25] or even square-pyramidal [25] structures. Coordination geometries at the midway between square pyramidal and trigonal bipyramidal have been described for zinc(II) complexes with tridentate Schiff base ligands [18]. A characteristic property of AH is the keto-enol tautomerism. In complexes the enolic form of the ligand is observable as is shown from the C–N (1.309, 1.313) and C–O (1.281) distances (C8–N1 and C8–O2). They are respectively shorter and longer than expected for the amide group [26]. Some other selected bond lengths and angles are shown in Table 4.

3.3. APX and AO mimicking studies

Ascorbate oxidase and ascorbate peroxidase are copper and iron containing metalloenzymes that are able to reduce molecular dioxygen or hydrogen peroxide to water in the presence of ascorbic acid as the electron donor [27–29]. AO is able to perform the reaction without the release of reactive oxygen species, while this is essential for APX. As a result, ascorbic acid (AA) is converted to dehydroascorbic acid (DHA) *via* single-electron-transfer mechanisms [6] (Fig. 2).

The reactivity of the metals determines the progression of the reactions in both cases. Although the trinuclear copper active site in AO [30] or the heme structure in APX [31] make our gly-AH – metal system considerably different from the enzymes, our aim was not to create structural models but to test this system in a model environment, where the presence of ROS is expected, and the ability of electron transfer is required. We carried out enzyme mimicking reactions in order to examine the behavior of the *in situ* generated Cu^{II}(gly-AH), Zn^{II}(gly-AH) and Fe^{III}(gly-AH) complexes as described above. Rate constants were determined under pseudo-first-order conditions ([ascorbic acid] = 10 × [ligand]), and the results are shown in Fig. 3. The observed average rate constants (k_{obs}) were compared with the complexes of the well known chelators ethylenediaminetetraacetic acid (EDTA) and desferrioxamine (DFO).

EDTA and the complexes of the title ligands show similar inhibition character. With all the metals in complex form the oxidation of AA is highly inhibited. The rate constants in case of copper drop from $k_{obs} = 1.43 \times 10^{-3}\ s^{-1}$ to $k_{obs} = 3.41 \times 10^{-5}\ s^{-1}$ with EDTA and $k_{obs} = 6.22 \times 10^{-6}\ s^{-1}$ with **L2**. The higher oxidation rate with DFO ($k_{obs} = 2.25 \times 10^{-4}\ s^{-1}$) can be explained either with the weak copper binding ability or with the stronger redox activity of the Cu–DFO complex. The H_2O_2 mediated oxidation of AA in the presence of iron is slower in our system ($k_{obs} = 1.66 \times 10^{-4}\ s^{-1}$). A 10-fold decrease is observable at the rate constants ($k_{obs} = 1.11 \times 10^{-5}\ s^{-1}$ and $k_{obs} = 3.62 \times 10^{-5}\ s^{-1}$) at inhibition by EDTA and gly-AH complexes. These results could be taken to indicate that the di-deprotonated gly-AH ligands are better chelates of copper(II) than iron(III) in solution.

Although zinc is not considered a redox active metal in its +2 oxidation state it still had a weak effect on AA oxidation and when complexed by addition of **L2** the reaction rate was almost 30-fold slower (from $k_{obs} = 7.11 \times 10^{-5}\ s^{-1}$ to $k_{obs} = 2.67 \times 10^{-6}\ s^{-1}$) than in non-complexed form. This reduction in rate was greater than was observed for iron while it was much smaller than in the case of copper. Fig. 3 clearly shows that the M^{II}(gly-AH) complexes were the most active in the prevention of ascorbic acid decomposition. We hypothesize that their activity may be due to the five and six-membered chelate ring system which enters into a redox cycle where the quenching of the ascorbate radical is more rapid than the autooxidation process (Scheme 2) and that the redox cycle is largely or wholly centered on the chelated ligand. Such behavior for similar ligands in association with non-redox active metals has previously been reported [32].

4. Conclusion

One approach that has been advocated for the treatment of neurodegenerative diseases, involves the application of chelators to remove elevated iron levels in brain. With this in mind we have prepared new lipophilic glyoxylato-aroylhydrazones possessing bulky aliphatic and glyoxylato moieties. Their structure and metal coordination characteristics were determined *via* their Cu and Zn complexes. The redox behavior of the complexes was investigated in a model environment, where the presence of ROS is expected to drive ascorbic acid decomposition.

Acknowledgments

This work has received funding by the Marie Curie Early Stage Research Training project "EURODESY" (Contract No. MEST-CT-020575) and the EU FP7-REGPOT-2009-1 project "ARCADE" (Grant Agreement 245866). We are grateful to Ms. Eleni Siapi for recording the ESI-MS spectra.

Appendix A. Supplementary data

CCDC 833643 and 833644 contain the supplementary crystallographic data for Cu(**L2**)$(Py)_2$ (**C1**) and Zn(**L2**)$(Py)_2$ (**C2**). These data can be obtained free of charge *via* http://www.ccdc.cam.ac.uk/conts/retrieving.html, or from the Cambridge Crystallographic Data Centre, 12 Union Road, Cambridge CB2 1EZ, UK; fax: (+44) 1223-336-033; or e-mail: deposit@ccdc.cam.ac.uk.

References

[1] S. Bolognin, D. Drago, L. Messori, P. Zatta, Med. Res. Rev. 29 (2009) 547.
[2] B.L. Vallee, K.H. Falchuk, Physiol. Rev. 73 (1993) 79.
[3] J.L. Buss, F.M. Torti, S.V. Torti, Curr. Med. Chem. 10 (2003) 1021.
[4] S.I. Liochev, I. Fridovich, Redox. Rep. 7 (2002) 55.
[5] A. Sigel, H. Sigel, R.K.O. Sigel, Metal Ions in Life Sciences, Neurodegenerative Diseases and Metal Ions, vol. 1, John Wiley & Sons Ltd., 2006. pp. 136.
[6] E.L. Raven, L. Lad, K.H. Sharp, M. Mewies, P.C.E. Moody, Biochem. Soc. Symp. 71 (2004) 27.
[7] L. Casella, E. Monzani, L. Santagostini, L. Gioia, M. Gullotti, P. Fantucci, T. Beringhelli, A. Marchesini, Coord. Chem. Rev. 185–186 (1999) 619.
[8] I. Yamazaki, L.H. Piette, Biochim. Biophys. Acta 50 (1961) 62.
[9] F. Arndt, Org. Synth. 2 (1943) 165.
[10] D.K. Johnson, T.B. Murphy, N.J. Rose, W.H. Goodwin, L. Pickart, Inorg. Chim. Acta 67 (1982) 159.
[11] Rigaku/MSC, CrystalClear, Rigaku/MSC Inc., The Woodlands, Texas, USA, 2005.

[12] G.M. Sheldrick, SHELXS-97: Structure Solving Program, University of Göttingen, Germany, 1997.
[13] G.M. Sheldrick, SHELXL-97: Crystal Structure Refinement Program, University of Göttingen, Germany, 1997.
[14] DIAMOND – Crystal and Molecular Structure Visualization, Ver. 3.1, Crystal Impact, Rathausgasse 30, 53111, Bonn, Germany.
[15] T.B. Chaston, D.B. Lovejoy, R.N. Watts, D.R. Richardson, Clin. Cancer Res. 9 (2003) 402.
[16] G. Link, P. Ponka, A.M. Konijn, W. Breuer, Z.I. Cabantchik, C. Hershko, Blood 101 (2003) 4172.
[17] F. Cariati, U. Caruso, R. Centore, W. Marcolli, A. De Maria, B. Panunzi, A. Roviello, A. Tuzi, Inorg. Chem. 41 (2002) 6597.
[18] A. Majumder, G.M. Rosair, A. Mallick, N. Chattopadhyay, S. Mitra, Polyhedron 25 (2006) 1753.
[19] S.N. Rao, D.D. Mishra, R.C. Maurya, N.N. Rao, Polyhedron 16 (1997) 1825.
[20] B.R. Steele, M. Micha- Screttas, C.G. Screttas, Appl. Organomet. Chem. 16 (2002) 501.
[21] B.N. Bessy Ray, M.R.P. Kurup, E. Suresh, Spectrochim. Acta Part A 71 (2008) 1253.
[22] K. Nakamoto, Infrared and Raman Spectra of Inorganic and Coordination Compounds, fourth ed., John Wiley & Sons Inc., 1986.
[23] A.W. Addison, T.N. Rao, J. Reedijk, J. van Rijn, G.C. Verschoor, J. Chem. Soc., Dalton Trans. (1984) 1349.
[24] N.M.H. Salem, A.R. Rashad, L. El-Sayed, W. Haase, M.F. Iskander, Polyhedron 28 (2009) 2137.
[25] F. Borbone, U. Caruso, R. Centore, A. De Maria, A. Fort, M. Fusco, B. Panunzi, A. Roviello, A. Tuzi, Eur. J. Inorg. Chem. (2004) 2467.
[26] F.H. Allen, O. Kennard, D.G. Watson, L. Brammer, A.G. Orpen, R. Taylor, J. Chem. Soc., Perkin Trans. 2 (1987) S1.
[27] M.C. De Tullio, R. Liso, O. Arrigoni, Biol. Plantarum 48 (2004) 161.
[28] V. Fotopoulos, M. Sanmartin, A.K. Kanellis, J. Exp. Botany 57 (2006) 3933.
[29] E.L. Raven, Subcell. Biochem. 35 (2000) 317.
[30] A. Messerschmidt, A. Rossi, R. Ladenstein, R. Huber, M. Bolognesi, G. Gatti, A. Marchesini, R. Petruzzelli, A. Finazzi-Agrò, J. Mol. Biol. 206 (1989) 513.
[31] W.R. Patterson, T.L. Poulos, Biochemistry 34 (1995) 4331.
[32] A.-G. Xie, Y. Qu, M.-M. Wang, G.-Q. Gan, H. Chen, Z.-D. Lin, D. Zhen, J. Coord. Chem. 62 (2009) 2268.